# A Powder Neutron Diffraction Investigation of the Two Rhombohedral NASICON Analogues: $\gamma$-$Na_3Fe_2(PO_4)_3$ and $Li_3Fe_2(PO_4)_3$

C. Masquelier,*,† C. Wurm,† J. Rodríguez-Carvajal,‡ J. Gaubicher,§ and L. Nazar§

*Laboratoire de Physicochimie des Solides, Université Paris-Sud, Bâtiment 414, 91405 Orsay Cedex, France, Laboratoire Léon Brillouin (CEA-CNRS), CEA/Saclay, 91191 Gif sur Yvette Cedex, France, and Department of Chemistry, University of Waterloo, Waterloo, Ontario N2L 3G1, Canada*

*Received September 6, 1999. Revised Manuscript Received October 22, 1999*

The crystal structures of polycrystalline rhombohedral $\gamma$-$Na_3Fe_2(PO_4)_3$ and $Li_3Fe_2(PO_4)_3$ obtained through Na ↔ Li ion exchange have been determined for the first time, from neutron diffraction data recorded at 473 and 300 K, respectively. $Na_3Fe_2(PO_4)_3$ crystallizes in the space group $R\bar{3}c$ at 473 K ($\gamma$-form, $a = 8.7270(2)$ Å, and $c = 21.8078(5)$ Å). A progressive transfer of $Na^+$ ions from the M(1) (6-coordinate) to the M(2) (8-coordinate) sites occurs upon raising the temperature from ambient (α-form, $\tau_{M(1)} = 1$) to 393 K ($\beta$-form, $\tau_{M(1)} = 0.91$) and then to 473 K ($\gamma$-form, $\tau_{M(1)} = 0.85$). This is associated with a significant increase of Fe−Fe distances through the M(1) site and with relaxation of the framework such that the $FeO_6$ octahedra become less distorted. Ion exchange from $Na_3Fe_2(PO_4)_3$ leads to the rhombohedral form of $Li_3Fe_2(PO_4)_3$ (space group $R\bar{3}$; $a = 8.3162(4)$ Å, and $c = 22.459(1)$ Å). The M(1) and M(2) sites of the NASICON structure are empty in $Li_3Fe_2(PO_4)_3$ which is isotypic with $Li_3In_2(PO_4)_3$. Removal of $Na^+$ from M(1) results in a strong increase of the *c* parameter due to stronger repulsions between adjacent $FeO_6$ octahedral faces along [001]. Lithium is located on one single-crystallographic site, M(3), with four Li−O distances ranging between 1.91 and 2.09 Å which span a regular tetrahedral geometry and gives rise to one signal in the $^6$Li spectrum at 152 ppm. Two crystallographic sites are clearly distinguished for iron: Fe(1)$O_6$ shares three of its vertexes only with $LiO_4$ tetrahedra and is far more distorted than Fe(2)$O_6$ which shares three edges with $LiO_4$ tetrahedra.

## Introduction

Three-dimensional polyanionic structures built of $XO_4^{n-}$ tetrahedra and $MO_6$ octahedra have been identified as interesting hosts for the reversible insertion of sodium or lithium.[1−18] Recent efforts have been devoted to the study of sulfates and phosphates of iron such as $Li_{1-x}FePO_4$ and $Li_xFe_2(SO_4)_3$ where reduction/oxidation of $Fe^{3+}/Fe^{2+}$ occurs at desirable potentials close to 3.5 V versus $Li/Li^+$.[4,8,14] Importantly, this potential can be "tuned" by modification to the substituents in the structure: for example, substitution of $PO_4^{3-}$ for $SO_4^{2-}$ in the "lantern unit" [$Fe_2(XO_4)_3$] shifts the $Fe^{3+}/Fe^{2+}$ redox couple by 0.8 eV through the inductive effect of the polyanion. A generalized mapping of transition-metal redox couples was recently proposed,[10] as a function of (1) the nature of the $XO_4^{n-}$ polyanion and (2) the connectivity between $FeO_6$ octahedra. $Li_3Fe_2(PO_4)_3$ was shown to reversibly intercalate two lithium ions at an average voltage of 2.8 V versus $Li/Li^+$ corresponding to the total reduction of $Fe^{3+}$ into $Fe^{2+}$.[8,17]

Depending on the preparation route, two distinct crystallographic forms of $Li_3Fe_2(PO_4)_3$ may be obtained,

* To whom correspondence should be addressed.
† Université Paris-Sud.
‡ CEA/Saclay.
§ University of Waterloo.

(1) Reiff, W. M.; Zhang, J. H.; Torardi, C. C. *J. Solid State Chem.* **1986**, *62*, 231−240.
(2) Manthiram, A.; Goodenough, J. B. *J. Solid State Chem.* **1987**, *71*, 349−360.
(3) Delmas, C.; Nadiri, A.; Soubeyroux, J. L. *Solid State Ionics* **1988**, *28−30*, 419−423.
(4) Manthiram, A.; Goodenough, J. B. *J. Power Sources* **1989**, *26*, 403−408.
(5) Tillement, O.; Couturier, J. C.; Angenault, J.; Quarton, M. *Solid State Ionics* **1991**, *48*, 249−255.
(6) Tillement, O.; Angenault, J.; Couturier, J. C.; Quarton, M. *Solid State Ionics* **1992**, *53−56*, 391−399.
(7) Boireau, A.; Soubeyroux, J. L.; Olazcuaga, R.; Delmas, C.; Le Flem, G. *Solid State Ionics* **1993**, *63−65*, 484−487.
(8) Okada, S.; Nanjundaswamy, K. S.; Manthiram, A.; Goodenough, J. B. Presented at the *36th Power Sources Conference*, June 6−9, 1994.
(9) Nanjundaswamy, K. S.; Padhi, A. K.; Goodenough, J. B.; Okada, S.; Ohtsuka, H.; Arai, H.; Yamaki, J. *Solid State Ionics* **1996**, *92*, 1−10.
(10) Goodenough, J. B.; Padhi, A. K.; Masquelier, C.; Nanjundaswamy, K. S.; Okada, S. *37th Battery Symposium*, Tokyo Institute of Technology, Tokyo, Japan, Sept 25−27, 1996.
(11) Znaidi, L.; Launay, S.; Quarton, M. *Solid State Ionics* **1997**, *93*, 273−277.
(12) Gaubicher, J.; Chabre, Y.; Angenault, J.; Lautié, A.; Quarton, M. *J. Alloys Compd.* **1997**, *262−263*, 34−38.
(13) Gaubicher, J.; Angenault, J.; Chabre, Y.; Le Mercier, T.; Quarton, M. *Mol. Cryst. Liquid Cryst.* **1998**, *311*, 45−49.
(14) Padhi, A. K.; Nanjundaswamy, K. S.; Goodenough, J. B. *J. Electrochem. Soc.* **1997**, *144*, 1188−1194.
(15) Padhi, A. K.; Nanjundaswamy, K. S.; Masquelier, C.; Okada, S.; Goodenough, J. B. *J. Electrochem. Soc.* **1997**, *144*, 1609−1613.
(16) Padhi, A. K.; Nanjundaswamy, K. S.; Masquelier, C.; Goodenough, J. B. *J. Electrochem. Soc.* **1997**, *144*, 2581−2586.
(17) Masquelier, C.; Padhi, A. K.; Nanjundaswamy, K. S.; Goodenough, J. B. *J. Solid State Chem.* **1998**, *135*, 228−234.
(18) Padhi, A. K.; Manivannan, V.; Goodenough, J. B. *J. Electrochem. Soc.* **1998**, *145*, 1518−1520.

10.1021/cm991138n CCC: $19.00 
Published on Web 01/13/2000

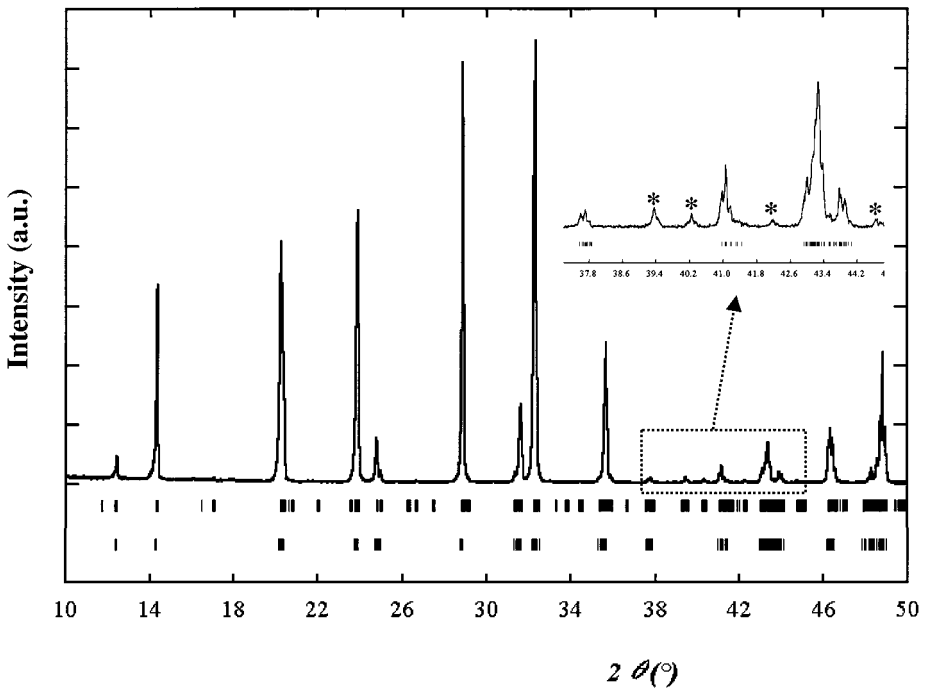


**Figure 1.** XRD Pattern (CuKα) of α-$Na_3Fe_2(PO_4)_3$. Bragg positions for the monoclinic subcell (below) and the superstructure monoclinic unit cell (upper) are indicated. Stars refer to the most intense superstructure reflections not indexed in the subcell.

which show distinct behavior upon Li intercalation.[17] $Li_3Fe_2(PO_4)_3$ can be prepared in a rhombohedral form through ion exchange from the NASICON sodium analogue $Na_3Fe_2(PO_4)_3$[21] and no structural work has been reported so far on that form. Our interest lies in determining the structural factors that impact the electrochemical behavior of the two polymorphs of $Li_3Fe_2(PO_4)_3$ upon lithiation, that is, for compositions $Li_{3+x}Fe_2(PO_4)_3$, $0 \leq x \leq 2$. Here, we report on detailed structural studies using neutron powder diffraction of the two rhombohedral NASICON $A_3Fe_2(PO_4)_3$ (A = Na, Li) compositions. The structure of the $\gamma$-form of $Na_3Fe_2(PO_4)_3$ was determined from data collected at 473 K. A comparison is drawn with the α- and $\beta$-forms previously reported,[22,23] which allows for a general discussion on NASICON framework modifications associated with the alkali ion transfer from M(1) to M(2) sites. This phenomenon is further supported by the study of the rhombohedral form of $Li_3Fe_2(PO_4)_3$ where both M(1) and M(2) sites are emptied.[24]

## Experimental Section

$Na_3Fe_2(PO_4)_3$ was prepared following the method of d'Yvoire,[21] through crystallization in a flux of sodium phosphates that leads to high-purity fine white powders. A mixture of $Fe_2O_3$ + 3.6 $NaH_2PO_4$ + 2.2 $Na_4P_2O_7$ was placed in a platinum crucible and heated to complete melting at 1193 K for 5 h. After cooling at 2 K/min, the solid was immersed in water and washed repeatedly to dissolve and remove the excess sodium phosphates. Rhombohedral $Li_3Fe_2(PO_4)_3$ was then prepared by three successive ion exchanges (1 day each) in a concentrated aqueous solution of $LiNO_3$ ($Li_{solution}/Na_{solid} > 10$). The phase purity was carefully monitored by X-ray diffraction on a Philips diffractometer (CuKα radiation) equipped with a graphite-diffracted beam monochromator.

Neutron diffraction experiments were performed at the Orphée reactor at the Laboratoire Léon Brillouin in Saclay, France. The neutron powder diffractometer G4.2 ($\lambda$ = 2.3433 Å) was used for a precise determination of the lattice parameters at room temperature of α-$Na_3Fe_2(PO_4)_3$ and $Li_3Fe_2(PO_4)_3$. The high-resolution neutron powder diffractometer 3T2 was used for data collection with high direct space resolution ($\lambda$ = 1.2251 Å; $Q_{max}$ = 9.2 $Å^{-1}$). The program FullProf was used for crystal structure refinements, employing the Rietveld method.[25,26]

## Results and Discussion

**Crystal Structures of $Na_3Fe_2(PO_4)_3$.** The X-ray diffraction pattern of α-$Na_3Fe_2(PO_4)_3$ recorded at room temperature is shown in Figure 1. Refinement using the monoclinic unit-cell, $a$ = 15.128(1) Å, $b$ = 8.721(1) Å, $c$ = 8.805(1) Å, and $\beta$ = 125.16(1)° in the space group $C2/c$ shows that small but clearly distinguishable diffraction peaks appear unindexed. They are the result of a superstructure cell presumably because of long-range sodium ordering on the M(1) and M(2) sites of the NASICON structure. These superstructure reflections were clearly identified by d'Yvoire et al. from a single-crystal study,[21,23] but never to our knowledge from a powder diffraction experiment. The true unit cell is then $a$ = 15.128(1) Å, $b$ = 8.721(1) Å, $c$ = 21.564(1) Å, and $\beta$ = 90.14(1)° in the probable space group $C2/c$. No detailed study of the superstructure has been published as of yet.

(19) Maksimov, B. A.; Muradyan, L. A.; Genkina, E. A.; Simonov, V. I. *Sov. Phys. Dokl.* **1986**, *31*, 370−372.
(20) Bykov, A. B.; Chirkin, A. P.; Demyanets, L. N.; Doronin, S. N.; Genkina, E. A.; Ivanov-Shits, A. K.; Kondratyuk, I. P.; Maksimov, B. A.; Mel'nikov, O. K.; Muradyan, L. N.; Simonov, V. I.; Timofeeva, V. A. *Solid State Ionics* **1990**, *38*, 31−52.
(21) d'Yvoire, F.; Pintard Scrépel, M.; Bretey, E.; de la Rochère, M. *Solid State Ionics* **1983**, *9/10*, 851−858.
(22) de la Rochère, M.; d'Yvoire, F.; Collin, G.; Comès, R.; Boilot, J. P. *Solid State Ionics* **1983**, *9/10*, 825−828.
(23) de la Rochère, M. Ph.D. Thesis, Université Pierre et Marie Curie Paris VI, Paris, France, 1984.
(24) Masquelier, C.; Rodriguez-Carvajal, J. Presented at the *12th International Conference on Solid State Ionics*, Thessaloniki, Greece, June 6−12, 1999.
(25) Rodriguez-Carvajal, J. *Physica B* **1993**, *192*, 55.
(26) Rietveld, H. M. *J. Appl. Crystallogr.* **1969**, *2*, 65.

**Table 1. Lattice Constants and Rietveld Refinement Results from Neutron Diffraction ($\lambda$ = 1.2251 Å) for γ-$Na_3Fe_2(PO_4)_3$ at 473 K and $Li_3Fe_2(PO_4)_3$ at 300 K**

| | γ-$Na_3Fe_2(PO_4)_3$ | $Li_3Fe_2(PO_4)_3$ |
|---|---|---|
| space group | $R\bar{3}c$ | $R\bar{3}$ |
| temperature | 473 K | 300 K |
| *a* | 8.7270(2) Å | 8.3162(4) Å |
| *c* | 21.8078(5) Å | 22.459(1) Å |
| *V*/*Z* | 239.73(1) Å$^3$ | 224.19(1) Å$^3$ |
| number of reflections | 529 | 989 |
| global refined parameters | 1 | 1 |
| profile refined parameters | 9 | 10 |
| int. dependent refined parameters | 20 | 33 |
| $R_P$ | 11.0% | 9.52% |
| $R_{wp}$ | 10.0% | 9.77% |
| $R_{exp}$ | 4.97% | 4.81% |
| $\chi^2$ | 4.02 | 4.13 |
| Bragg *R* factor | 6.94% | 3.50% |

It is well-known that $Na_3Fe_2(PO_4)_3$ undergoes two reversible phase transitions: α ↔ β at 368 K and β ↔ γ at 418 K[21,27] related to order/disorder rearrangements on the sodium sites within the $[Fe_2(PO_4)_3]\infty$ framework. In the average description of the structure of the room-temperature form (α), the occupation factors of the NASICON M(1) and M(2) alkali sites are 1 and $^2/_3$, respectively,[22,23] but the exact nature of the ordered-sodium distribution in the supercell is still unknown. The crystal structure of the β-form at 393 K was also determined: compared to the room-temperature form α, there is an important transfer of $Na^+$ ions from the Na(1) site to the Na(2) site, their occupation factors becoming 0.91(2) and 0.70(2), respectively, but with persistence of long-range ordering on the Na(2) sites.[22] There are no structural data reported so far on the rhombohedral form γ of $Na_3Fe_2(PO_4)_3$.

We have determined the crystal structure of γ-$Na_3Fe_2(PO_4)_3$ using neutron diffraction ($\lambda$ = 1.2251 Å) at 473 K on a powder sample, far above the β → γ phase transition. Profile-matching refinements gave lattice parameters *a* = 8.727(1) Å and *c* = 21.807(1) Å in space group $R\bar{3}c$, in very good agreement with those obtained from X-ray data.[22] Note that there is a substantial increase in the *c* parameter as the temperature is raised (*c* = 21.569(3) Å in the pseudohexagonal α-form; *c* = 21.733(5) Å in the β-form). The atomic coordinates of γ-$Na_3Cr_2(PO_4)_3$ in space group $R\bar{3}c$[23] were used as the starting model for the Rietveld refinements, for which the initial occupancy factors on the Na(1) and Na(2) sites were taken to be equal to those of the β-form. The refinement converged rapidly to satisfactory agreement factors and the thermal parameters to reasonable values. The thermal parameters on the Na(1) and Na(2) sites were refined first with the occupation factors kept equal to those of the α-form. Then, the isotropic temperature factors were kept constant to allow refinement of the occupation factors for which the sum was constrained to lead to 3 Na per formula unit. A significant improvement of the crystal structure was then obtained by refining the anisotropic thermal parameters on the Na(1) and Na(2) sites. The final agreement factors are listed in Table 1, and the list of fractional coordinates is given in Table 2. Selected interatomic distances and angles are compared with the corresponding data of the α- and β-forms in Table 3.

**Table 2. Atomic Coordinates of γ-$Na_3Fe_2(PO_4)_3$ and Anisotropic Temperature Factors ($\beta_{ij}$) of the Na Sites**

| atom | *x* | *y* | *z* | $B_{eq}$ | occ. |
|---|---|---|---|---|---|
| Na(1) | 0 | 0 | 0 | 0[a] | 0.85(3) |
| Na(2) | 0.6348(8) | 0 | 0.25000(0) | 0[a] | 0.72(3) |
| Fe | 0 | 0 | 0.14874(5) | 0.85(2) | 1 |
| P | 0.2902(2) | 0 | 0.25000(0) | 1.14(3) | 1 |
| O(1) | 0.1793(2) | −0.0267(2) | 0.19370(7) | 2.34(3) | 1 |
| O(2) | 0.1911(2) | 0.1685(2) | 0.08892(5) | 1.53(2) | 1 |

| atom | $B_{11}$ | $B_{22}$ | $B_{33}$ | $B_{12}$ | $B_{13}$ | $B_{23}$ |
|---|---|---|---|---|---|---|
| Na(1) | 1084(106) | 1084(106) | 0.3(1.8) | 1084(106) | 0.0 | 0.0 |
| Na(2) | 146(13) | 98(12) | 63(3) | 98(12) | 19(5) | 39(5) |

[a] Refined anisotropically.

**Table 3. Selected Interatomic Distances in $Na_3Fe_2(PO_4)_3$[a]**

| | | α | | | β | γ |
|---|---|---|---|---|---|---|
| **Fe** | O(5) | 1.944(3) | **Fe** | O(1) ×3 | 1.952(4) | 1.956(2) |
| | O(2) | 1.955(4) | | O(2) ×3 | 2.048(2) | 2.048(2) |
| | O(4) | 1.959(5) | | | | |
| | O(3) | 2.042(2) | | | | |
| | O(1) | 2.053(3) | | | | |
| | O(6) | 2.055(4) | | | | |
| | | **2.001** | | | **2.000** | **2.002** |
| P(1) | O(4) | 1.527(5 | | | | |
| | O(1) | 1.527(3) | | | | |
| | O(5) | 1.528(3) | **P** | O(1) ×2 | 1.526(3) | 1.508(2) |
| | O(3) | 1.535(4) | | O(2) ×2 | 1.533(2) | 1.541(2) |
| | | **1.529** | | | **1.529** | **1.525** |
| **P(2)** | O(2) ×2 | 1.521(4) | | | | |
| | O(6) ×2 | 1.532(3) | | | | |
| | | **1.526** | | | | |
| Na(1) | O(3) ×2 | 2.436(4) | **Na(1)** | O(2) ×6 | 2.480(2) | 2.500(1) |
| | O(6) ×2 | 2.440(2) | | | **2.480** | **2.500** |
| | O(1) ×2 | 2.457(3) | | | | |
| | | **2.444** | **Na(2)** | O(2) ×2 | 2.391(3) | 2.384(2) |
| **Na(2′)** | O(1) ×2 | 2.394(4) | | O(2) ×2 | 2.448(4) | 2.453(6) |
| | O(6) ×2 | 2.428(2) | | O(1) ×2 | 2.619(3) | 2.642(2) |
| | O(5) ×2 | 2.591(4) | | O(1) ×2 | 2.854(4) | 2.839(5) |
| | O(4) ×2 | 2.897(4) | | | **2.578** | **2.579** |
| | | **2.577** | | | | |
| **Na(3′)** | O(6) | 2.366(4) | | | | |
| | O(3) | 2.415(4) | | | | |
| | O(3) | 2.438(4) | | | | |
| | O(1) | 2.471(5) | | | | |
| | O(4) | 2.531(4) | | | | |
| | O(2) | 2.633(5) | | | | |
| | O(2) | 2.827(8) | | | | |
| | O(5) | 2.889(4) | | | | |
| | | **2.571** | | | | |

[a] Average distances are indicated in bold characters; data for the α- and β-forms are taken from refs 22 and 23.

The structure is entirely described in the space group $R\bar{3}c$ using the 6 independent atomic positions of the NASICON structure. The framework is built of $[Fe_2(PO_4)_3]$ "lantern units" stacked parallel to the [001] direction (Figure 2). The local symmetries around Fe and P are 3 and 2, respectively, with Fe−O and P−O average bond lengths (Table 3) characteristic of $Fe^{3+}$ and $P^{5+}$ in octahedral and tetrahedral coordination environments, respectively. The sodium ions are distributed over two crystallographic sites. The point symmetry of the 6-coordinate M(1) that lies along [001], between two $[Fe_2(PO_4)_3]$ lantern units is 3. The point symmetry of M(2) is 2; it is 8-coordinated and lies at the same *z* value as the phosphorus atom.

One first interesting phenomenon in the structure of γ-$Na_3Fe_2(PO_4)_3$ lies in the values of the occupation

(27) Pintard-Scrépel, M.; d'Yvoire, F.; Rémy, F. *C. R. Acad. Sci. Paris* **1978**, *286*, 381−383.

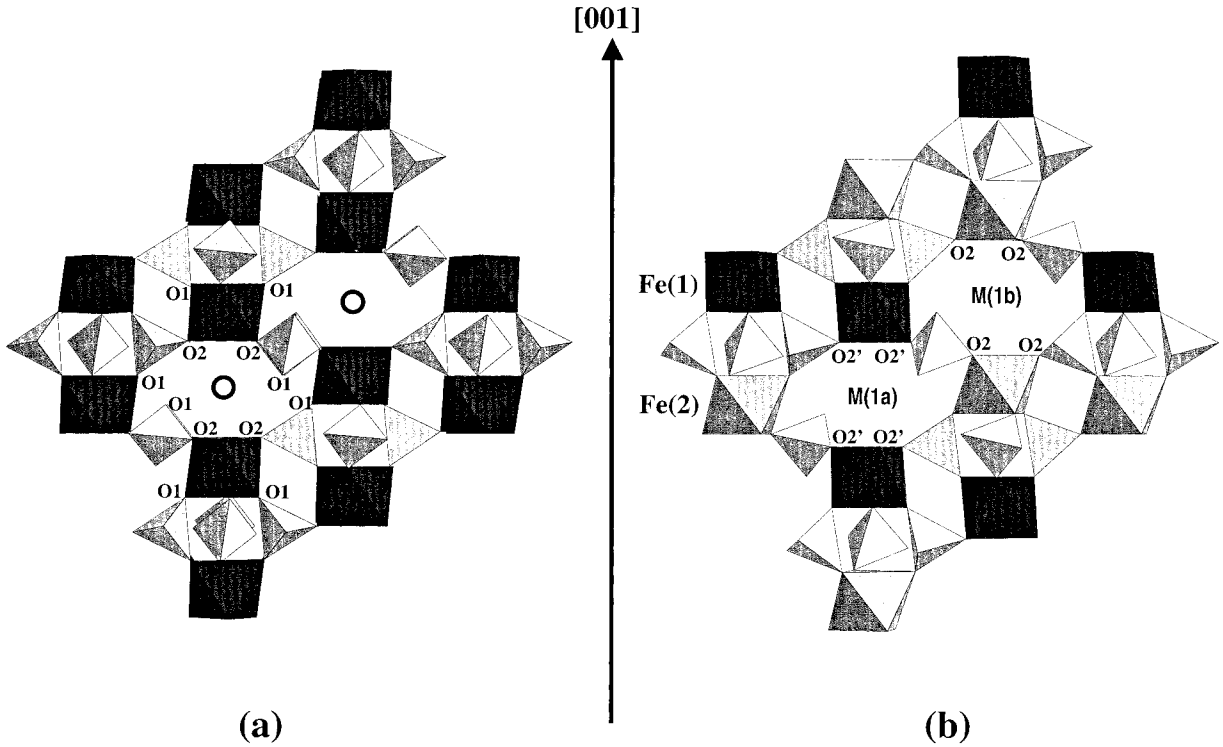


**Figure 2.** NASICON frameworks in (a) $\gamma$-$Na_3Fe_2(PO_4)_3$ and (b) $Li_3Fe_2(PO_4)_3$. O refers to the M(1) position.

factors that we found for the Na(1) and Na(2) sites, 0.85(3) and 0.72(3), respectively. They vary significantly from those found for the α-form (room temperature) and $\beta$-form (393 K). Thus, the global transfer from Na atoms from Na(1) to the Na(2) sites upon increasing temperature, observed for $Na_3M_2(PO_4)_3$ (M = Sc, Cr),[22] is also confirmed for $Na_3Fe_2(PO_4)_3$. This rearrangement induces several minor but significant changes in the NASICON framework. The size of the Na(1) antiprismatic cavity is increased as it is depopulated and this has a direct impact on the value of the *c* parameter as (i) the size of the $FeO_6$ octahedron remains essentially the same and (ii) the Fe−Fe distance within the lantern unit along [001] (4.417 Å) is unchanged. On the other hand, the Fe−Fe distance through the Na(1) site along [001] increases from 6.451 Å in the $\beta$-form to 6.487 Å in the $\gamma$-form. The fractional coordinate *z* of O(2) increases regularly when the value of the occupancy factor $\tau_{M(1)}$ of the Na(1) site decreases, as can be seen in Figure 3a. This coordinate is indeed a direct measure of the height of the Na(1) cavity, given by $2 \times z_{O(2)} \times c$.

The second interesting feature lies in the geometry of the $FeO_6$ octahedron which, because of strong electrostatic repulsion between $Na^+$ in the Na(1) site and $Fe^{3+}$, is notably distorted in the α-form. As shown in Figure 3b, the trends observed by de la Rochère during the α → $\beta$ transition[23] still prevail for the $\gamma$-form of $Na_3Fe_2(PO_4)_3$: when the Na(1) site is progressively depopulated, the $FeO_6$ octahedron becomes less distorted as the O−Fe−O angles shift to values closer to 90°. Within the $FeO_6$ octahedron, O(1) and O(2) sites play clearly distinct roles. O(2) constitutes the octahedral M(1) cavity between adjacent $Fe_2(PO_4)_3$ lantern units along [001], while O(1) constitutes the empty ("internal") cavity located between the two $FeO_6$ octahedra of the $Fe_2(PO_4)_3$ lantern unit (Figure 2). It follows that the Fe−O(2) bond lengths are much longer (2.048 Å) than those

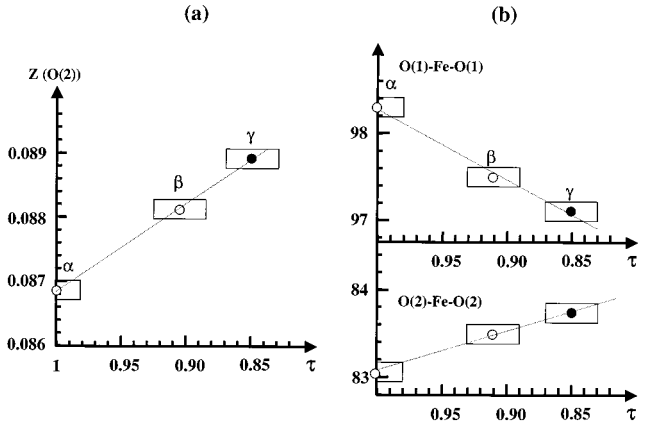


**Figure 3.** Evolution of the NASICON framework distortion with the occupancy of the M(1) site in $Na_3Fe_2(PO_4)_3$. White circles: data from refs 22 and 23. Black circles: this study.

of Fe−O(1) (1.956 Å) while the O(2)−Fe−O(2) angle (83.8°) is lower than the O(1)−Fe-O(1) angle (97.1°). Examination of the Fe−Fe distances along [001] shows that the increase in the *c* parameter on going from α → $\beta$ → $\gamma$ is only due to the increase of the M(1) cavity height as it is progressively depopulated: the Fe−Fe distance within the lantern unit remains the same as that in the $\beta$-form (4.417(2) Å) while the Fe−Fe distance through the M(1) cavity increases from 6.449(2) Å in the $\beta$-form to 6.487(2) Å in the $\gamma$-form.

**Crystal Structure of $Li_3Fe_2(PO_4)_3$ (Rhombohedral $R\bar{3}$).** Ion exchange of $Na_3Fe_2(PO_4)_3$ in a concentrated $LiNO_3$ solution allows the preparation of a $Li_3Fe_2(PO_4)_3$ composition where the relative positions of the $[Fe_2(PO_4)_3]$ lantern units are those of the NASICON structure, in contrast to that observed for the monoclinic ($P2_1/n$) form.[21] The X-ray diffraction pattern presented in Figure 4 is fully indexed with lattice parameters $a$ = 8.309(1) Å and $c$ = 22.462(1) Å in the

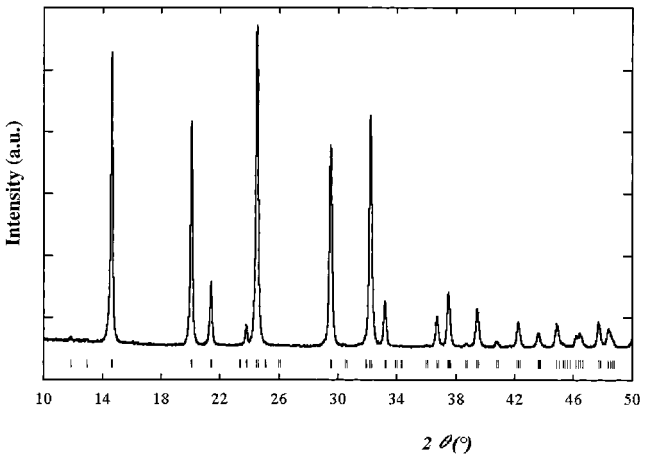


**Figure 4.** XRD Pattern (CuKα) of $Li_3Fe_2(PO_4)_3$ indexed in the space group $R\bar{3}$.

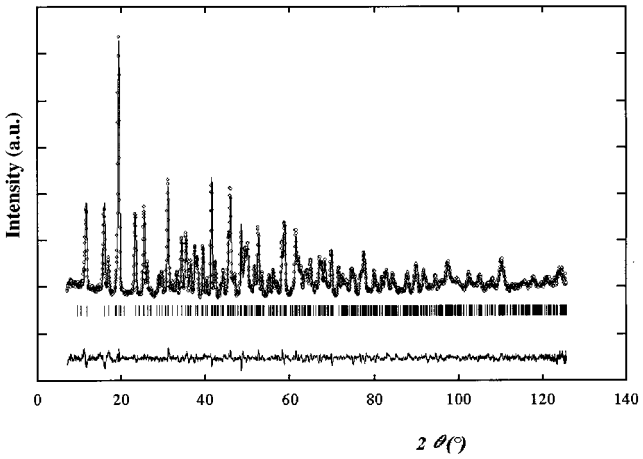


**Figure 5.** Observed and calculated powder neutron diffraction patterns of $Li_3Fe_2(PO_4)_3$ ($\lambda = 1.2251$ Å).

**Table 4. X-ray Powder Diffraction Data for Rhombohedral $Li_3Fe_2(PO_4)_3$ at Room Temperature**

| *h* | *k* | *l* | *d* (Å) | $I/I_{max}$ (%) | $I_{calc}$ |
|---|---|---|---|---|---|
| 0 | 0 | 3 | 7.487 | 2 | 6 |
| 1 | 0 | 1 | 6.853 | 2 | 11 |
| 0 | 1 | 2 | 6.059 | 78 | 100 |
| 1 | 0 | 4 | 4.427 | 61 | 98 |
| 2 | −1 | 0 | 4.155 | 20 | 22 |
| 1 | 1 | 0 | | | |
| 0 | 0 | 6 | 3.744 | 5 | 8 |
| 2 | −1 | 3 | 3.633 | 100 | 141 |
| 1 | 1 | 3 | | | |
| 2 | 0 | 2 | 3.427 | 1 | 1 |
| 0 | 2 | 4 | 3.030 | 68 | 70 |
| 2 | −1 | 6 | 2.781 | 80 | 103 |
| 1 | 1 | 6 | | | |
| 3 | −1 | 1 | 2.700 | 16 | 23 |
| 2 | 1 | 1 | | | |
| 3 | −1 | 4 | 2.448 | 11 | 18 |
| 2 | 1 | 4 | | | |
| 0 | 3 | 0 | 2.399 | 10 | 31 |
| 0 | 2 | 7 | 2.395 | 2 | 4 |
| 3 | 0 | 3 | 2.284 | 8 | 22 |
| 2 | 0 | 8 | 2.214 | 3 | 2 |
| 2 | −1 | 9 | 2.139 | 11 | 16 |
| 1 | 1 | 9 | | | |
| 3 | −1 | 7 | 2.075 | 5 | 7 |
| 2 | 1 | 7 | | | |
| 0 | 3 | 6 | 2.020 | 5 | 9 |
| 4 | −1 | 2 | 1.965 | 3 | 8 |
| 3 | 1 | 2 | | | |
| 0 | 1 | 11 | 1.964 | 2 | 1 |
| 3 | −2 | 8 | 1.954 | 5 | 7 |
| 1 | 2 | 8 | | | |
| 0 | 2 | 10 | 1.905 | 10 | 17 |
| 4 | −3 | 4 | 1.881 | 8 | 13 |
| 1 | 3 | 4 | | | |
| 0 | 0 | 12 | 1.872 | 3 | 4 |

space group $R\bar{3}$. The indexed powder X-ray diffraction data are given in Table 4. The presence of the (303) reflection at $2\theta = 39.45°$ definitely rules out the space group $R\bar{3}c$ previously proposed.[21,17] Note the very strong increase in the *c* parameter as $Na^+$ is replaced by $Li^+$. From the previous discussion on γ-$Na_3Fe_2(PO_4)_3$ it follows that there might be a global redistribution of lithium within the framework, in particular, owing to the smaller size of $Li^+$ that does not favor occupation of the large 6- and 8-coordinated M(1) and M(2) cavities.

The lattice parameters of $Li_3Fe_2(PO_4)_3$ determined from powder neutron diffraction ($\lambda = 1.2251$ Å) are $a = 8.3162(4)$ Å and $c = 22.459(1)$ Å in the space group $R\bar{3}$. An initial series of Rietveld refinements was undertaken by using the atomic coordinates of γ-$Na_3Fe_2(PO_4)_3$ ($R\bar{3}c$) transformed in the space group $R\bar{3}$, including lithium in positions derived from the Na(1) and Na(2) sites of the NASICON structure. It became immediately obvious that the occupation of these sites by lithium was very unlikely. Instead, we used the fractional coordinates of $Li_3In_2(PO_4)_3$ reported by Genkina,[28] which crystallizes also in the space group $R\bar{3}$, as the starting model for the Rietveld refinements. As we shall describe in detail, we found that $Li_3Fe_2(PO_4)_3$ is indeed isotypic with $Li_3In_2(PO_4)_3$[28] and that the alkali cations that reside on the Na(1) and Na(2) sites of $Na_3Fe_2(PO_4)_3$ are redistributed on a new 4-fold-coordinated site that we label M(3) in $Li_3Fe_2(PO_4)_3$. The experimental, calculated, and difference profiles are given in Figure 5. The final agreement factors, fractional coordinates, and selected interatomic distances and angles are given in Tables 1, 5, and 6, respectively. The loss in symmetry on going from the space group $R\bar{3}c$ for γ-$Na_3Fe_2(PO_4)_3$ to $R\bar{3}$ for $Li_3Fe_2(PO_4)_3$ induces a splitting of the unique iron site of the sodium analogue to two independent iron sites, Fe(1) and Fe(2), that still lie on the 3-fold axis (Figure 2). There is still one unique crystallographic site for P and each of the 2 oxygen sites of the sodium analogue is split into two independent sites, O(*i*) and O(*i*′). The M(1) site of γ-$Na_3Fe_2(PO_4)_3$ also splits into two M(1a) and M(1b) sites, both unoccupied in $Li_3Fe_2(PO_4)_3$ but that should be differentiated in respect to further discussion on Li location in the structure.

*Lithium Environment.* The most important feature of the crystal structure of rhombohedral $Li_3Fe_2(PO_4)_3$ is that the 6-coordinated M(1) site of the NASICON structure is empty. This is no surprise, indeed, as this cavity in α-$Na_3Fe_2(PO_4)_3$ is far too big (Na(1)−O = 2.44 Å) to sustain the smaller $Li^+$ ion. Following the general trend observed through the transitions $\alpha \rightarrow \beta \rightarrow \gamma$ in $Na_3Fe_2(PO_4)_3$, there is thus a strong increase in the *c* parameter when M(1) is depopulated. This phenomenon has been previously discussed on going from $LiTi_2(PO_4)_3$

(28) Genkina, E. A.; Muradyan, L. A.; Maksimov, B. A.; Merinov, B. V.; Sigarev, S. E. *Sov. Phys. Crystallogr.* **1987**, *32*, 40−42.
(29) Brown, I. D.; Altermatt, D. *Acta Crystallogr.* **1985**, *B41*, 244.
(30) Masquelier, C.; Wurm, C.; Gaubicher, J.; Goward, G.; Nazar, L. Submitted for publication.
(31) Salinas-Sanchez, A.; Garcia-Munoz, J. L.; Rodriguez-Carvajal, J.; Saez-Puche, R.; Martinez, J. L. *J. Solid State Chem.* **1992**, *100*, 201−211.

**Table 5. Atomic Coordinates of $Li_3Fe_2(PO_4)_3$ and Anisotropic Temperature Factors ($\beta_{ij}$) on the Li Site**

| atom | *x* | *y* | *z* | *B* | occ. |
|---|---|---|---|---|---|
| Fe(1) | 0 | 0 | 0.1461(2) | 0.28(5) | 1 |
| Fe(2) | 0 | 0 | 0.6528(2) | 0.31(5) | 1 |
| P | 0.2923(4) | 0.0019(5) | 0.2513(2) | 0.32(4) | 1 |
| O(1) | 0.1915(6) | −0.0096(6) | 0.1919(2) | 2.49(9) | 1 |
| O(1′) | 0.7656(5) | 0.9126(5) | 0.6990(1) | 1.44(6) | 1 |
| O(2) | 0.2434(5) | −0.1993(5) | 0.2659(2) | 1.36(7) | 1 |
| O(2′) | 0.5006(4) | 0.8796(5) | 0.7556(2) | 1.10(6) | 1 |
| Li(3) | 0.341(2) | 0.024(2) | 0.3819(6) | 0[a] | 1 |

| atom | $B_{11}$ | $B_{22}$ | $B_{33}$ | $B_{12}$ | $B_{13}$ | $B_{23}$ |
|---|---|---|---|---|---|---|
| Li(3) | 212(31) | 331(46) | 12(3) | 297(36) | 9(9) | −3(10) |

[a] Refined anisotropically.

to $Li_3Ti_2(PO_4)_3$.[3] In the latter material, the M(1) site is also reported to be empty but no complete structural study has been reported so far. By analogy to what we have found for $Li_3Fe_2(PO_4)_3$, we suspect that, in $Li_3Ti_2(PO_4)_3$, the M(2) site should not be occupied either. In $Li_3Fe_2(PO_4)_3$, lithium occupies one crystallographic site in the general position (18f) of $R\bar{3}$ which we call M(3). This site is not the M(2) site of the NASICON structure (8-coordinated) but is slightly shifted (∼±0.8 Å) along [001] and lies in a fairly regular tetrahedral coordination with an average Li−O distance of 2.03 Å (Table 6). This favors total occupancy and the relatively small value of the isotropic thermal parameter indicates that lithium is somewhat localized in this cavity, although mobility may still be higher than that in the monoclinic phase, A-$Li_3Fe_2(PO_4)_3$ as suggested by a comparative study of ionic conductivity in both A- and B-forms of $Li_3Cr_2(PO_4)_3$.[21]

The location of Li in a single site in the lattice is also confirmed by our solid-state MAS $^{6,7}$Li NMR studies. Spectra were acquired at 4.68 T to minimize paramagnetic relaxation effects, using natural abundance $^6$Li NMR which affords better spectral resolution, although this necessitated a long spectral acquisition time. The M(3) tetrahedral $LiO_4$ site exhibits a single resonance at 162 ppm similar to that in isostructural $Li_3V_2(PO_4)_3$ where the corresponding $^6$Li shift for Li occupation in M(3) is observed at 88 ppm.[30]

MAS NMR investigations of rhombohedral $Li_3Fe_2(PO_4)_3$ were also carried out with $^7$Li (to facilitate more rapid spectral acquisition). Spectra of $Li_3Fe_2(PO_4)_3$ were characterized by very rapid decay in the time domain, suggesting that rapid relaxation behavior occurs for Li in these sites. This is due to a combination of paramagnetic relaxation as a result of through-space $^7$Li coupling to the electron spin on the $Fe^{3+}$ ion and/or spin-relaxation effects due to Li mobility. Comparison to the monoclinic phase (space group $P2_1/n$) of $Li_3Fe_2(PO_4)_3$, which has similar $Li^+-Fe^{3+}$ distances, suggests that paramagnetic interaction is not the only effect however, as there were still very noticeable differences in the relaxation behavior that must be related to differences in ion hopping in the structures. Work is in progress to investigate this in detail.

*Lithium Distribution within the Framework*. A close examination of the relative positions of the lithium ions within the framework was undertaken. The results are shown in Figures 6−8. The $Li^+$ ions are arranged in layers perpendicular to [001] and are related to each other by the inversion centers of $R\bar{3}$. These layers are

**Table 6. Selected Interatomic Distances (Å) and Angles (deg) in $Li_3Fe_2(PO_4)_3$[a]**

| Fe(1) | O(1) | O(1) | O(1) | O(2′) | O(2′) | O(2′) |
|---|---|---|---|---|---|---|
| O(1) | **1.929(6)** | 94.3(4) | 94.3(4) | 98.6(3) | 166.8(4) | 82.5(3) |
| O(1) | 2.83(7) | **1.929(6)** | 94.3(4) | 82.5(3) | 98.6(3) | 166.8(4) |
| O(1) | 2.83(7) | 2.83(7) | **1.929(6)** | 166.8(4) | 82.5(3) | 98.6(3) |
| O(2′) | 3.03(6) | 2.63(6) | 3.96(7) | **2.063(5)** | 85.4(3) | 85.4(3) |
| O(2′) | 3.96(7) | 3.03(6) | 2.63(6) | 2.80(5) | **2.063(5)** | 85.4(3) |
| O(2′) | 2.63(6) | 3.96(7) | 3.03(6) | 2.80(5) | 2.80(5) | **2.063(5)** |

⟨Fe−O⟩ = 1.996(5) Å; predict. = 2.016 Å; $\Delta = 113 \times 10^{-5}$; $V_{sum} = 3.21$

| Fe(2) | O(1′) | O(1′) | O(1′) | O(2) | O(2) | O(2) |
|---|---|---|---|---|---|---|
| O(1′) | **1.996(5)** | 95.5(3) | 95.5(3) | 87.0(3) | 89.2(3) | 174.5(4) |
| O(1′) | 2.95(7) | **1.996(5)** | 95.5(3) | 174.5(4) | 87.0(3) | 89.2(3) |
| O(1′) | 2.95(7) | 2.95(7) | **1.996(5)** | 89.2(3) | 174.5(4) | 87.0(3) |
| O(2) | 2.76(5) | 4.02(6) | 2.83(5) | **2.020(5)** | 88.1(3) | 88.1(3) |
| O(2) | 2.83(5) | 2.76(5) | 4.02(6) | 2.82(5) | **2.020(5)** | 88.1(3) |
| O(2) | 4.02(6) | 2.83(5) | 2.76(5) | 2.82(5) | 2.82(5) | **2.020(5)** |

⟨Fe−O⟩ = 2.008(5) Å; predict. = 2.016 Å; $\Delta = 4 \times 10^{-5}$; $V_{sum} = 3.06$

| P | O(1) | O(1′) | O(2) | O(2′) |
|---|---|---|---|---|
| O(1) | **1.555(7)** | 111.8(5) | 105.8(5) | 110.9(5) |
| O(1′) | 2.55(6) | **1.524(6)** | 112.1(4) | 107.3(5) |
| O(2) | 2.48(6) | 2.55(5) | **1.548(5)** | 109.0(4) |
| O(2′) | 2.52(7) | 2.44(6) | 2.49(6) | **1.505(6)** |

⟨P−O⟩ = 1.533(5) Å; predict. = 1.534 Å; $\Delta = 17 \times 10^{-5}$; $V_{sum} = 5.03$

| Li(3) | O(1′) | O(1′) | O(2) | O(2′) |
|---|---|---|---|---|
| O(1′) | **1.92(2)** | 113.2(7) | 115.3(8) | 124.2(7) |
| O(1′) | 3.44(6) | **2.20(2)** | 84.9(7) | 97.2(6) |
| O(2) | 3.21(6) | 2.76(5) | **1.88(2)** | 115.3(7) |
| O(2′) | 3.57(5) | 3.24(5) | 3.33(5) | **2.11(2)** |

⟨Li−O⟩ = 2.028(5) Å; predict. = 1.979 Å; $\Delta = 434 \times 10^{-5}$; $V_{sum} = 0.93$

[a] The M−O distances are underlined. O−O distances are given below the diagonal and O−M-O angles are given above. The bond valence sum ($V_{sum}$) is calculated using the Zachariasen formula: $V_i = \sum_j s_{ij} = \sum_j \exp\{(d_0 - d_{ij})/0.37\}$ using the parameters $d_0$, characterizing a cation−anion pair, from ref 29. The distortion parameter $\Delta$ of a coordination polyhedron $MO_N$ with an average M−O distance $\langle d \rangle$ is defined as $\Delta = (1/N)\sum_{n=1,N} \{(d_n - \langle d \rangle)/\langle d \rangle\}^2$.

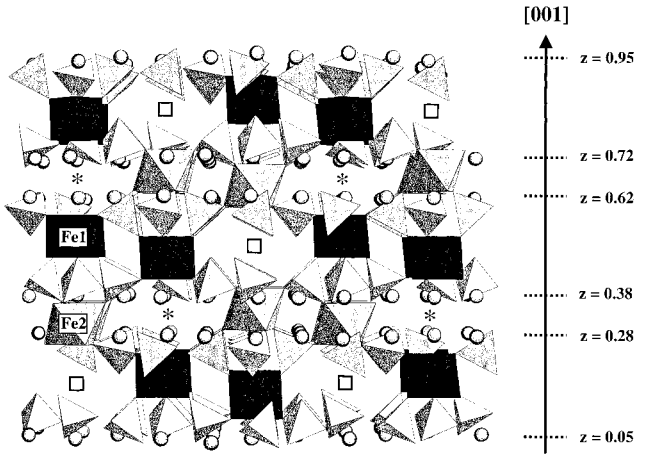


**Figure 6.** Crystal structure of $Li_3Fe_2(PO_4)_3$. Projection along [110]. $Fe(1)O_6$ octahedra are darkened compared to $Fe(2)O_6$ octahedra. Lithium atoms are represented by circles. The stars and squares refer to emptied M(1a) and M(1b) positions of the $Na_3Fe_2(PO_4)_3$ analogue, respectively.

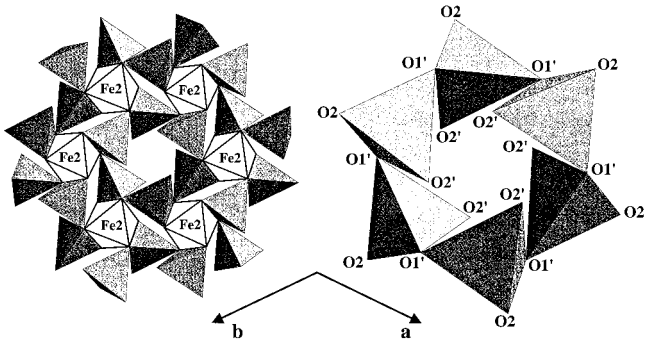


**Figure 7.** Crystal structure of $Li_3Fe_2(PO_4)_3$: projection along [001] showing the $Li_6O_{18}$ "rings" linked through the edges to $Fe(2)O_6$ octahedra.

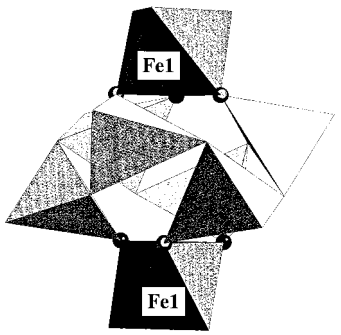


**Figure 8.** Crystal structure of $Li_3Fe_2(PO_4)_3$: two $Fe(1)O_6$ octahedra connected to a $Li_6O_{18}$ ring through O(2′).

grouped by "pairs" (at $z = 0.28$ and $z = 0.38$, for instance) that represent the actual shifts of lithium ions along [001], compared to the M(2) positions of $Na_3Fe_2(PO_4)_3$ that are regularly spaced at the same fractional coordinates as the phosphorus atoms along $z$ ($z = 0.25$ and $z = 0.42$, respectively). As seen in Figure 6, the M(1a) and M(1b) sites derived from one single M(1) site of the $R\bar{3}c$ structure are clearly distinguished here. They are both empty but each pair of layers surrounds one M(1a) site and not an M(1b) site. As is evident in Figure 7, the lithium ions that belong to the same pair of layers (hence related to each other by the 3 operation on M(1a)), form 6-membered rings of $LiO_4$ tetrahedra linked to each other through the oxygen atom O(1′). The 6 oxygen atoms O(2′) of a given $Li_6O_{18}$ ring all belong to the *empty* $M(1a)O_6$ elongated octahedron; thus, each $LiO_4$ tetrahedron shares one corner with the $Fe(1)O_6$ octahedron. Figure 7 also clearly indicates that each $LiO_4$ tetrahedron shares an edge (O(2)−O(1′)) with a given $Fe(2)O_6$ octahedron. Within an $Li_6O_{18}$ ring, each lithium is surrounded by two lithiums at 3.36(2) Å. The Li−Li shortest distance between neighboring $Li_6O_{18}$ rings, on the other hand, is 3.78(2) Å. The lithium distribution, is thus fairly regular and seems to represent an electrostatic ordering onto fully occupied well-defined crystallographic positions. This suggests that there may be an effect on the ionic conductivity in this particular form of the NASICON structure; the peculiar "bilayered" arrangement of the lithium positions could restrict it to being two-dimensional in character. The values of the anisotropic thermal factors that were successfully refined for the Li site fully support this assumption (Table 5): they are far more important within the (**a,b**) plane than along the [001] direction.

*Iron Environment.* The peculiar distribution of lithium within the framework generates different constraints on the $Fe(1)O_6$ and $Fe(2)O_6$ octahedra. These two sites, equivalent in $R\bar{3}c$, are independent in $Li_3Fe_2(PO_4)_3$ as a result of different Li environments. As seen in Figure 8, $Fe(1)O_6$ shares three of its corners (O(2′)) with three different $LiO_4$ tetrahedra. On the contrary, $Fe(2)O_6$ shares all its corners (O(1′) and O(2)), through three edges in common, with three different $LiO_4$ tetrahedra (Figure 7). This results in very different bond-lengths distributions and distortions in these two octahedra (Table 6) as indicated by a bond valence calculation. The very good quality of the refinement is further supported by the quite low (0.14) global instability index, defined in ref 31. In $Fe(1)O_6$, the three Fe−O(2′) bonds (with oxygen that also belongs to $LiO_4$ tetrahedra) are far much longer (2.063(5) Å) than the three Fe−O(1) ones (1.929(6) Å) as O(2′)s participate in Li coordination, but O(1) does not. $Fe(2)O_6$, which is regularly surrounded by Li, on the contrary, is much less distorted. As already discussed for the sodium analogue, depopulation of the M(1) site in the NASICON framework results in a strong increase of the $c$ parameter. We distinguished, in the previous section, two Fe−Fe distances along [001] depending on whether the iron atoms belong to the same lantern unit or not (4.417(2) and 6.487(2) Å). Here, because of the loss of $R\bar{3}c$ symmetry, there are three Fe−Fe distances along [001] and the $c$ parameter decomposes according to the following sequence: Fe(1)−Fe(2) (4.515(5) Å) + Fe(2)−Fe(2) (6.865(5) Å) + Fe(2)−Fe(1) (4.515(5) Å) + Fe(1)−Fe(1) (6.564(5) Å) (Figure 6). The strongest repulsion occurs therefore between Fe(2) and Fe(2) adjacent octahedral faces that are not "screened" by alkali cations, that is, through the empty M(1b) cavity (Figure 6). One notes, however, that the Fe(1)−Fe(2) distance within a lantern unit is also significantly increased too (∼+0.1 Å) and this might cause some structural instability that would favor the transformation to the monoclinic ($P2_1/n$) stable form of $Li_3Fe_2(PO_4)_3$.

## Conclusion

This study represents the first step of our global research on the structural behavior of three-dimensional

polyanionic frameworks based on the NASICON structure: $Li_{3\pm x}M_2(PO_4)_3$ (M = Fe, V). By examining the same fundamental structure type, $A_3Fe_2(PO_4)_3$, where A = Li, Na, and the phase changes that occur with temperature, we obtained structural results that revealed the exceptional flexibility of the NASICON framework $MM'(XO_4)_3$ and demonstrated that the nature of the alkali cation also plays a major role in effecting changes to the framework structure. These detailed studies are also important in the context of alkali insertion or extraction during electrochemical redox processes because these materials are viable positive electrode materials in Li batteries. For example, insertion of 2 lithium (reduction of $Fe^{3+}$ into $Fe^{2+}$) in rhombohedral $Li_3Fe_2(PO_4)_3$ was recently demonstrated.[17] Ex situ experiments suggest that the resulting 5 lithium ions are accommodated within the same NASICON framework.[32] Future work will focus on structural and electrochemical studies of this insertion process, and on the corresponding extraction process from the isostructural compound $Li_3V_2(PO_4)_3$.

(32) Gaubicher, J. et al. Unpublished results.

**Acknowledgment.** We are grateful to Prof. Clare Grey (SUNY Stony Brook) for helpful discussions and NMR spectral acquisition at variable fields and to Gillian Goward (University of Waterloo) and Dr. Hiltrud Grondey (University of Toronto) for their help. L.F.N. acknowleges NSERC (Canada) for financial support through the Research Grants Program. C.M. gratefully thanks Prof. Ferdinand d'Yvoire for extremely valuable discussions.

CM991138N